

SATO: Stable Text-to-Motion Framework

Wenshuo Chen*
Shandong University
Qingdao, China
chatoncws@gmail.com

Hongru Xiao*
Tongji University
Shanghai, China
hongru_xiao@tongji.edu.cn

Erhang Zhang*
Shandong University
Qingdao, China
seve19861@gmail.com

Lijie Hu
King Abdullah University
of Science and Technology
Jeddah, Saudi Arabia
lijie.hu@kaust.edu.sa

Lei Wang
Australian National
University & Data61/CSIRO
Canberra, Australia
lei.w@anu.edu.au

Mengyuan Liu
State Key Laboratory of
General Artificial
Intelligence, Peking
University, Shenzhen
Graduate School
Shenzhen, China
nkliuyifang@gmail.com

Chen Chen
Center for Research in
Computer Vision,
University of Central
Florida
Orlando, USA
chen.chen@crcv.ucf.edu

Abstract

Is the Text to Motion model robust? Recent advancements in Text to Motion models primarily stem from more accurate predictions of specific actions. However, the text modality typically relies solely on pre-trained Contrastive Language-Image Pretraining (CLIP) models. Our research has uncovered a significant issue with the text-to-motion model: its predictions often exhibit inconsistent outputs, resulting in vastly different or even incorrect poses when presented with semantically similar or identical text inputs. In this paper, we undertake an analysis to elucidate the underlying causes of this instability, establishing a clear link between the unpredictability of model outputs and the erratic attention patterns of the text encoder module. Consequently, we introduce a formal framework aimed at addressing this issue, which we term the **Stable Text-to-Motion Framework (SATO)**. SATO consists of three modules, each dedicated to stable attention, stable prediction, and maintaining a balance between accuracy and robustness trade-off. We present a methodology for constructing an SATO that satisfies the stability of attention and prediction. To verify the stability of the model, we introduced a new textual synonym perturbation dataset based on HumanML3D and KIT-ML. Results show that SATO is significantly more stable against synonyms and other slight perturbations while keeping its high accuracy performance. Codes and models are released at <https://github.com/sato-team/Stable-Text-to-Motion-Framework>

CCS Concepts

• **Computing methodologies** → **Computer vision**.

*represents equal contribution

Permission to make digital or hard copies of all or part of this work for personal or classroom use is granted without fee provided that copies are not made or distributed for profit or commercial advantage and that copies bear this notice and the full citation on the first page. Copyrights for components of this work owned by others than the author(s) must be honored. Abstracting with credit is permitted. To copy otherwise, or republish, to post on servers or to redistribute to lists, requires prior specific permission and/or a fee. Request permissions from permissions@acm.org.

MM '24, October 28–November 1, 2024, Melbourne, VIC, Australia

© 2024 Copyright held by the owner/author(s). Publication rights licensed to ACM.

ACM ISBN 979-8-4007-0686-8/24/10

<https://doi.org/10.1145/3664647.3681034>

Keywords

Human Motion Generation, Stable Text-to-Motion Framework, Robustness

ACM Reference Format:

Wenshuo Chen, Hongru Xiao, Erhang Zhang, Lijie Hu, Lei Wang, Mengyuan Liu, and Chen Chen. 2024. SATO: Stable Text-to-Motion Framework. In *Proceedings of the 32nd ACM International Conference on Multimedia (MM '24)*, October 28–November 1, 2024, Melbourne, VIC, Australia. ACM, New York, NY, USA, 14 pages. <https://doi.org/10.1145/3664647.3681034>

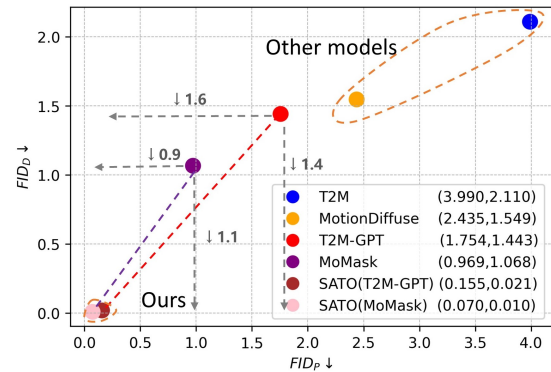


Figure 1: Comparisons on FID_D and FID_P . The closer the model is to the origin, the better. The arrow indicates the effect of our method on the model. Our SATO framework can make the text-to-motion model more stable.

1 Introduction

The Text-to-Motion (T2M) model signifies a groundbreaking and swiftly advancing paradigm with immense potential across various domains, such as video games, the metaverse, and virtual or augmented reality environments. This innovative approach, as evidenced by research contributions from [6, 7, 9, 33, 38, 41] revolves around generating motion data directly from textual descriptions, thereby simplifying the overall process and mitigating associated time and cost overheads.

However, a fundamental challenge inherent in text-to-motion tasks stems from the variability of textual inputs [39]. Even when

conveying similar or the same meanings and intentions, texts can exhibit considerable variations in vocabulary and structure due to individual user preferences or linguistic nuances. Despite the considerable advancements made in these models, we find a notable weakness: all of them demonstrate instability in prediction when encountering minor textual perturbations, such as synonym substitutions (examples and comparisons are shown in Fig. 4). This is a serious issue. The instability of the model leads to **inconsistent outputs, with errors in details or even entirely incorrect** motion sequence, when users input synonymous or closely related sentences. This limitation confines our model research within a narrow range of expressions, hindering the future development and practical applications of text-to-motion models.

This prompts us to inquire: **What are the root causes of these issues? Are they rooted in inadequacies in textual modalities, language comprehension, or their harmonization?** Through posing these questions, elucidating this problem, and striving for a robust text-to-motion framework emerges as an urgent necessity.

Most text-to-motion models build upon pre-trained text encoders, such as CLIP [28]. Previous works have shown discrepancies in downstream tasks utilizing CLIP text encoders despite similar semantic inputs [16]. Further investigation reveals that similar phenomena occur in the text-to-motion domain. Taking the T2M-GPT [38] model as an example, several experimental findings emerge. First, we observed a close correlation between instability attention and incorrect prediction outcomes (shown in Fig. 4). Differences in attention can lead to significant disparities in text feature representations during intermediate processes. Secondly, in many instances, by rectifying the initial token of inaccurately predicted action sequences, subsequent accurate action sequences were obtained (see Fig. 2). Lastly, the initial motion sequence token was predicted based on the text feature. Significant differences in the first motion sequence token can lead to significant variations in the first motion sequence token. We further elucidate the aforementioned experimental findings: When perturbed text is inputted, the model exhibits unstable attention, often neglecting critical text elements necessary for accurate motion prediction. This instability further complicates the encoding of text into consistent embeddings, leading to a cascade of consecutive temporal motion generation errors. **Notably, the stability of the model manifests in the consistency of textual attention, highlighting its pivotal role in mitigating such errors.**

For a more robust text-to-motion framework, we must delve into what constitutes stability, meaning requiring us to define stability for the text-to-motion model. Intuitively, a stable attention and prediction text-to-motion model should possess the following three properties for any text input:

- Considering from a bionics perspective, it should possess a stable attention mechanism, focusing on key motion descriptions without changing with synonym perturbation.
- Its prediction distribution should exhibit stability, i.e., robustness to synonym or near-synonym substitution replacement perturbations during training and testing.
- Its prediction distribution closely resembles that of the original model in inputs without perturbation, ensuring outstanding performance.

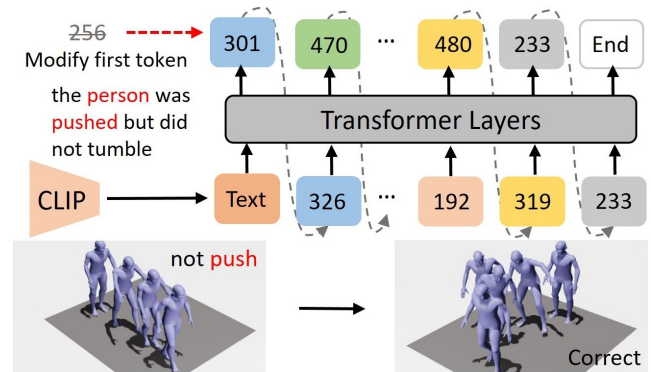


Figure 2: Token modification example. In many examples, when the input is perturbed, the model produces an incorrect motion sequence, as shown in the bottom-left figure. When we correct the first erroneous token during the model prediction process, we obtain the correct motion sequence, as depicted in the bottom-right figure. The accuracy of the first token is crucial for the subsequent temporal predictions of the model.

For the first two criteria, as discussed earlier, we work on stabilizing the model’s attention and predictions, both indirectly and directly, to stabilize the overall results. As for the last criterion, we emphasize the trade-off between model stability and accuracy. We aim for the model to maintain its excellent performance as much as possible. Based on these criteria, this paper presents a formal definition of a stable attention and robust prediction framework called SATO (Stable Text-to-Motion Framework).

To assess better robustness, we construct a large dataset of synonym perturbations based on two widely used datasets: KIT-ML [27] and HumanML3D [8]. It is noteworthy that even when not utilized specifically for stability tasks, our perturbed text dataset can still serve as valuable data augmentation to enhance model performance. Empirically, SATO achieves comparable performance to state-of-the-art models while demonstrating superior stability, as illustrated in Fig. 1. Extensive experimentation on these benchmark datasets, employing T2M-GPT and Momask models for verification, underscores the effectiveness of our approach. Our results reveal that we achieve optimal stability while maintaining accuracy (e.g., on T2M-GPT, HumanML3D dataset original text FID 0.157 vs **0.141**, perturbed text FID **0.155** vs. 1.754). Moreover, human evaluation results indicate a significantly reduced catastrophic error rate post-perturbation in contrast to the SOTA models, while also suggesting a subjective preference for the outputs generated by our model. In conclusion, our contributions can be summarized as follows:

- To the best of our knowledge, this is the first work to discover the instability issue in text-to-motion models. Our work formulates a formal and mathematical definition for a stable text-to-motion framework named SATO, proposes a dataset for measuring stability, and establishes relevant evaluation metrics, laying the foundation for improving the stability of text-to-motion models.
- Through extensive experimentation, we validate the effectiveness of our approach, showcasing its superiority in handling textual perturbations with comparable performance and higher stability. Additionally, we successfully strike a balance between accuracy

and stability, ensuring our model maintains high precision even in the face of perturbations.

- Our work points to a novel direction for improving text-to-motion models, paving the way for the development of more robust models for real-world applications.

2 RELATED WORK

2.1 Text-conditioned human motion generation

Text-conditioned human motion generation aims to generate 3D human actions based on textual descriptions. Recent mainstream work can be divided into two categories, namely VAE-based methods and diffusion models. VAE [1, 4, 5, 30, 34, 36] has achieved excellent performance in multi-modal generation tasks. ACTOR [25] proposes a Transformer-based VAE for generating motion from predefined action categories. TEMOS [26] introduces an additional text encoder based on ACTOR for generating different motion sequences based on text descriptions, but mainly focusing on short sentences. Guo et al. [8] propose an autoregressive conditional VAE conditioned on the generated frame and text features, and proposed to predict motions based on the length of the text. TEACH [2] is based on TEMOS, which generates temporal motion combinations from a series of natural language descriptions and extends space for long motion combinations. TM2T [9] considers not only text-to-motion tasks, but also motion-to-text tasks, and the joint training of these two tasks will be improved. T2M-GPT [38] quantizes motion clips into discrete markers and then uses a converter to generate subsequent markers. However, whether it is the diffusion-based method [22, 33, 41] the VAE-based method, or even previous work such as MotionCLIP [32], the structure is based on the CLIP encoder [20]. When the text is subject to slight perturbation, the model may exhibit inconsistent outputs, even leading to catastrophic errors in motion, which is a common and severe problem with these past methods.

2.2 Robustness of text conditioned motion generation

For the stabilization of input vector perturbations, some work has been done on stabilizing the output pattern of the model from various perspectives. Reconstructing the perturbed text with the actual input text can improve the the robustness of the text model [31], but does not guarantee the model’s attention similarity before and after the perturbation. Shunsuke et al. [17] enhance the text embedding stability using adversarial learning but do not analyze the consistency between old and new attention, making it difficult to ensure that textual attention can have consistent results for different descriptive scenarios under the same semantics. In text-to-motion field, Wang et al. [35] introduced a multi-layer graph neural network to learn the local features and correlations of tokens in action descriptions. Jin et al. [15] constructed a hierarchical semantic graph to enrich the details of action generation while maintaining the overall coherence of the actions.

However, for multidimensional descriptions that the text embedding model has not encountered, the inherent challenge lies in the static text model’s difficulty in reading characteristic description information, making it hard for the model to align the semantic features of descriptions across different dimensions [21]. Therefore, we need to pay attention to the consistency of textual attention

before and after the description perturbation. And we also pay attention to the local importance and overall compatibility of semantic weights, to avoid the repeated generation of the emphasized part of the description, thus ignoring the coherence of the whole action.

3 METHOD

3.1 Preliminaries

Vanilla Attention. For text embedding, Text-to-Motion mainly uses CLIP or other text vector models [6] to encode the action description text. For the original description text, tokenization is first performed to obtain the token index vector, i.e., $\mathbf{t} \in \mathbb{R}^{n \times 1}$, where n represents the number of tokens. Next, the token will be embedded by the embedding weights, i.e. $\mathbf{e} \in \mathbb{R}^{V \times d}$, where V is the size of vocab, d is the dimension of the embedding vectors. Therefore, when \mathbf{t} goes through the embedding layer, it can obtain the corresponding embedded expression based on the token index, which is notated as $\mathbf{t}_e \in \mathbb{R}^{n \times d}$. Attention weight is to express the relationship between the query and the key, here we use Scaled Dot-Product to calculate its correlation, which is $a(\mathbf{q}, \mathbf{k}) = \text{softmax}\left(\frac{\mathbf{q}\mathbf{k}^T}{\sqrt{d}}\right) \in \mathbb{R}^{n \times m}$, where $\mathbf{k} \in \mathbb{R}^{m \times d}$ and $\mathbf{q} \in \mathbb{R}^{n \times d}$. Finally, the correlation weight is multiplied by $\mathbf{v} \in \mathbb{R}^{m \times v}$ to get the output $\mathbb{R}^{n \times v}$. Additionally, the tensors are divided into multi-heads, thus the corresponding final attention weights obtained are also the average between the individual heads, i.e. $\omega_t = \frac{1}{h} \sum_{i=1}^h a(\mathbf{q}, \mathbf{k})_i \in \mathbb{R}^{n \times m}$.

VQ-VAE Based Text-to-Motion Model. Our objective is to produce a 3D human pose sequence $\mathbf{X} = [\mathbf{x}_1, \mathbf{x}_2, \dots, \mathbf{x}_T]$, where $\mathbf{x}_t \in \mathbb{R}^d$, guided by a textual description $\mathbf{C} = [c_1, c_2, \dots, c_l]$, where T represents the number of frames and d denotes the dimension of the motion feature. Here, c_i represents the i^{th} word in the sentence, and l is the length of the sentence. The process begins with extracting a text embedding \mathbf{c}_e from input text using CLIP. Subsequently, a transformer model predicts the distribution of possible next indices $p(S_i | \mathbf{c}_e, S_{<i})$ based on the text embedding \mathbf{c}_e and previous indices $S_{<i}$, where S_i represents the index of the next element at position i in the sequence. These predicted indices are then mapped to corresponding entries in the learned codebook, yielding latent code representations $\hat{\mathbf{z}}_i$ [34]. Finally, the decoder network decodes these codebook entries into motion sequences \mathbf{X}_{pred} . The optimization objective aims to maximize the log-likelihood of the data distribution. This is achieved by denoting the likelihood of the full sequence as $p(S | \mathbf{c}_e) = \prod_{i=1}^{|S|} p(S_i | \mathbf{c}_e, S_{<i})$ and directly maximizing it: $\mathcal{L}_{\text{trans}} = \mathbb{E}_{S \sim p(S)} [-\log p(S | \mathbf{c}_e)]$ [3, 7, 38], facilitating the generation of motion sequences from input text.

Perturbations for Texts. To introduce effective perturbation methods for text, we consider a scenario where a perturbation $C = [c_1, c_2, \dots, c_l]$ is applied to transform the original text into $C' = [c'_1, c'_2, \dots, c'_l]$ or perturbing the text embedding c to c' . Several strategies have been shown to be effective in prior works, such as Greedy Coordinate Gradient (GCG) [42], Projected Gradient Descent [24] (PGD). However, due to the inherent diversity of user inputs and the presence of noise in sentences, we incorporate two distinct perturbation techniques in this study: Projected Gradient Descent (PGD) and Random Synonym Replacement (RSR). PGD finds the perturbation direction along the steepest ascent in the loss landscape, while

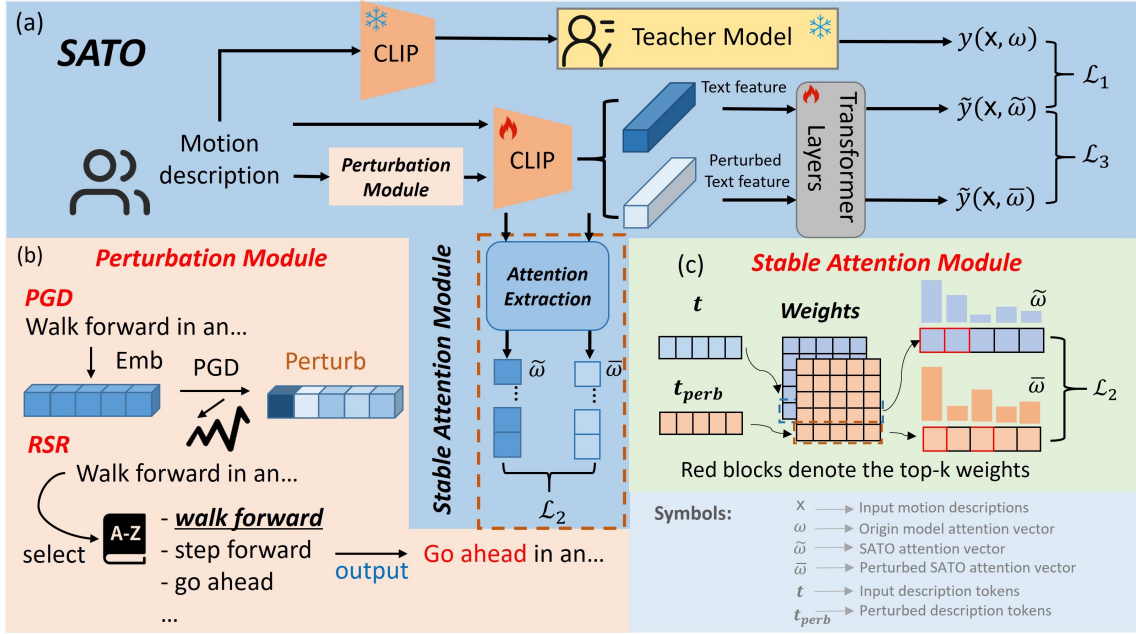


Figure 3: (a) Framework of our proposed Stable Text-to-Motion (SATO). It comprises three components: perturbation module, stable attention module, and pretrained teacher model. (b) The perturbation module encompasses two approaches for perturbation, namely Random Synonym Replacement (RSR) and Projected Gradient Descent (PGD). This module is utilized to emulate various perturbations encountered during user interactions. (c) The stable attention module aligns the top-k attention index weights before and after perturbation to stabilize the model’s attention distribution. Additionally, we incorporate a frozen teacher module, solely utilized during training, to stabilize the model’s motion generation capability, thus balancing the trade-off between accuracy and robustness.

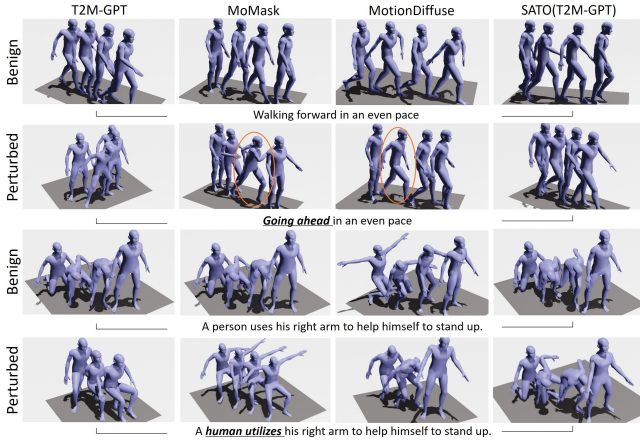


Figure 4: Visual results on user testing. SATO (T2M-GPT) refers to fine-tuning based on T2M-GPT to create SATO. Below each action sequence is the corresponding motion caption. The bold text represents the top-k attention weight words. It can be seen that the perturbation of the caption can lead to changes in the attention of the text, which can lead to catastrophic errors in the generative model. SATO has demonstrated superior stability to other models both in terms of attention and motion prediction.

RSR is done manually through human-designed synonym perturbations. These approaches are chosen to address the variability in user inputs and to tackle the challenges posed by noisy sentences.

By employing PGD or RSR perturbations, we aim to enhance the robustness of our text-processing techniques against diverse inputs and noise.

3.2 Problem Formulation

The Stability Issue in Text-to-motion Models. The pre-trained CLIP model used as a text encoder for text-to-motion tasks has inherent limitations in maintaining stable attention for semantically similar or identical sentences, while minor perturbations are inevitable during user input. Furthermore, text-to-motion models generally lack the stable capability to handle perturbed text embeddings, leading to inconsistent predictions despite similar or identical semantic inputs. This instability renders it unsuitable for real-world applications where robustness and reliability are crucial. Addressing these issues requires us to analyze them from different perspectives.

Attention Stability. We first present the definition of the top-k overlap ratio for two vectors [11]. For vector $\mathbf{x} \in \mathbb{R}^n$, we define the set of top-k components $T_k(\cdot)$ as:

$$T_k(\mathbf{x}) = \{i : i \in [d] \text{ and } |\{x_j \geq x_i : j \in [n]\}| \leq k\}.$$

For two vectors \mathbf{x}, \mathbf{x}' , their top-k overlap ratio $V_k(\mathbf{x}, \mathbf{x}')$ is denoted as:

$$V_k(\mathbf{x}, \mathbf{x}') = \frac{1}{k \cdot |T_k(\mathbf{x}) \cap T_k(\mathbf{x}')|} \quad (1)$$

For the original text input, we can easily observe the model’s attention vector for the text. This attention vector reflects the model’s

attentional ranking of the text, indicating the importance of each word to the text encoder’s prediction. We hope a stable attention vector maintains a consistent ranking even after perturbations. For a piece of text, demanding all attention magnitudes to be similar is overly strict. For instance, in "Walking forward in an even pace", the words "Walking", "forward", and "even" should have the most significant impact on the motion sequence. Therefore, we relax the requirement and only demand that the top-k indices remain unchanged.

Prediction Robustness. Even with stable attention, we still cannot achieve stable results due to the change in text embeddings when facing perturbations, even with similar attention vectors. This requires us to impose further restrictions on the model’s predictions. Specifically, in the face of perturbations, the model’s prediction should remain consistent with the original distribution, meaning the model’s output should be robust to perturbations.

Balancing Accuracy and Robustness. Accuracy and robustness are naturally in a trade-off relationship [12, 18, 19, 29, 37]. Our objective is to bolster stability while minimizing the decline in model accuracy, thereby mitigating catastrophic errors arising from input perturbations. Consequently, we require a mechanism to uphold the model’s performance concerning the original input.

Let $y(\mathbf{x})$ denote the prediction of the original text-to-motion model, and ω denote the attention vector. Based on the discussion above, we introduce the Stable Text-to-Motion Framework (SATO) with modified prediction \tilde{y} and attention vector $\tilde{\omega}$ as follows:

- (1) **(Prediction Robustness)** $D_1(\tilde{y}(\mathbf{x}, \tilde{\omega}), \tilde{y}(\mathbf{x}, \tilde{\omega} + \boldsymbol{\rho}_1)) \leq \gamma_1$, for some $\|\boldsymbol{\rho}_1\| \leq R_1, \gamma_1 \geq 0$.
- (2) **(Closeness of Prediction)** $D_2(\tilde{y}(\mathbf{x}, \tilde{\omega}), y(\mathbf{x}, \omega)) \leq \gamma_2$, for some $\gamma_2 \geq 0$.
- (3) **(Top-k Attention Robustness)** $V_k(\tilde{\omega}, \tilde{\omega} + \boldsymbol{\rho}_2) \geq \beta$, for some $1 \geq \beta \geq 0, \|\boldsymbol{\rho}_2\| \leq R_2$.

Specifically, $\boldsymbol{\rho}_1$ and $\boldsymbol{\rho}_2$ represent perturbations; R_1 and R_2 is the robust radius, which measures the robust region; D_1 and D_2 are metrics of the similarity between two distributions, which could be a distance or a divergence; γ_1 measures the robustness of prediction while γ_2 measures the closeness of the two prediction distributions; $0 < \beta < 1$ is the robustness of top-k indices. When β is larger, then the attention module will be more robust; $\|\cdot\|$ is \mathcal{L}_1 or \mathcal{L}_2 norm.

It is worth noting that the roles of Prediction Robustness and Top-k Robustness are not redundant. For instance, consider the vectors $\mathbf{v}_1 = (0.2, 0.1, \mathbf{0.4}, \mathbf{0.7})$ and $\mathbf{v}_2 = (0.3, 0.5, \mathbf{0.8}, \mathbf{1.0})$, which have the same top indices. However, the difference in their magnitudes can significantly affect the final prediction. The former affects the robustness of the prediction, while the latter emphasizes the stability of the attention vector. From a bionics perspective, the latter facilitates the model to more stably focus on crucial motion information.

3.3 Stable Text-to-Motion Framework

We have already proposed a rigorous definition of SATO. To build our framework (shown in Fig. 3), we based SATO on T2M-GPT [38]. Our emphasis lies in highlighting SATO as a plug-and-play framework adaptable to all current methodologies employing a combination of text encoders and transformer layers. We conducted thorough experiments on SATO utilizing T2M-GPT as our foundational model, enriching our analysis. Furthermore, we validated

SATO’s feasibility within the MoMask [7]. To obtain a text encoder module with more stable attention, we unfreeze the CLIP module, which was originally frozen in most of the work [7, 38], and derive a minimum-maximum optimization problem with three conditions from the above three mathematical formulas, as shown in the following formula.

$$\min_{\tilde{\mathcal{W}}} \mathbb{E}_{\mathbf{x}} [\lambda_1 (D_2(\tilde{y}(\mathbf{x}, \tilde{\omega}), y(\mathbf{x}, \omega)) - \gamma_2) + \max_{\|\boldsymbol{\rho}\| \leq R} \lambda_2 (\beta - V_k(\tilde{\omega}, \tilde{\omega} + \boldsymbol{\rho})) + \lambda_3 (\max_{\|\boldsymbol{\rho}\| \leq R} D_1(\tilde{y}(\mathbf{x}, \tilde{\omega}), \tilde{y}(\mathbf{x}, \tilde{\omega} + \boldsymbol{\rho})) - \gamma_1)] \quad (2)$$

where $\lambda_1, \lambda_2, \lambda_3$ are hyperparameters, $\tilde{\mathcal{W}}$ represents the weight of the model. Here, we employ a maximum perturbation $\boldsymbol{\rho}$ that acts simultaneously on both factors. We need to point out that there are two challenges in the optimization: (1) **How to handle the non-differentiable function** $-V_k(\tilde{\omega}, \tilde{\omega} + \boldsymbol{\rho})$, and (2) **how to find $\boldsymbol{\rho}$ that maximizes the perturbation on ω within a certain range.**

Stable Attention Module. For the first issue, we need to seek an equivalent $\mathcal{L}_{\text{Topk}}$ to replace $-V_k(\tilde{\omega}, \tilde{\omega} + \boldsymbol{\rho})$. The previous discussion highlighted the necessity of considering the overlap of the previous k indices for the stability of our attention mechanism. This implies that solely relying on \mathcal{L}_1 -norm or \mathcal{L}_2 -norm is insufficient [11]. We need a method that is both differentiable and ensures attention to the top-k indices. One approach is to introduce the cross-distance of the values associated with the top-k indices for computation. Here, we introduce a loose surrogate loss:

$$\mathcal{L}_{\text{Topk}} = \frac{1}{2k} (\|\omega_{\zeta_k^\omega} - \tilde{\omega}_{\zeta_k^\omega}\| + \|\tilde{\omega}_{\zeta_k^{\tilde{\omega}}} - \omega_{\zeta_k^{\tilde{\omega}}}\|) \quad (3)$$

where ζ_k^ω represents the top-k indices set of vector ω , and $\|\cdot\|$ denotes a norm. In this paper, the \mathcal{L}_1 -norm is used, which yields the best experimental results. This definition serves two purposes: it ensures the stability of the top-k indices of attention and cleverly resolves the non-differentiability issue. We have $\omega = (0.1, \mathbf{0.3}, \mathbf{0.7})$ and $\tilde{\omega} = (\mathbf{0.5}, 0.1, \mathbf{0.2})$. We use the top-2 indices, denoted as $\zeta_2^\omega = [1, 2]$ and $\zeta_2^{\tilde{\omega}} = [0, 1]$. Using the \mathcal{L}_1 -norm, we obtain $\mathcal{L}_{\text{Top2}} = \frac{1}{4} (|[0.3, 0.7] - [0.1, 0.2]| + |[0.1, 0.3] - [0.5, 0.1]|) = 0.325$.

Perturbation Module. Regarding the second issue, one approach is to introduce artificially generated high-quality synonym perturbation datasets, thereby obtaining the maximum perturbation for $\tilde{\omega}$. And for another approach, we interpret it as maximizing its susceptibility to attack for seeking the maximum perturbation for $\tilde{\omega}$. We transform this problem into solving the minimal max-attack within a certain range. Through the process of PGD [24] with n iterations, we search for the maximum attack $\boldsymbol{\rho}$.

$$\boldsymbol{\rho}_k = \boldsymbol{\rho}_{k-1}^* + \frac{r_k}{|\mathcal{B}_n|} \sum_{x \in \mathcal{B}_n} \nabla (D_2(y(x, \tilde{\omega}), y(x, \tilde{\omega} + \boldsymbol{\rho}_{k-1}^*))) + \mathcal{L}_{\text{Topk}}(\omega, \tilde{\omega} + \boldsymbol{\rho}_{k-1}^*) \quad (4)$$

$$\boldsymbol{\rho}_k^* = \operatorname{argmin}_{\|\boldsymbol{\rho}\| \leq R} \|\boldsymbol{\rho} - \boldsymbol{\rho}_k\|$$

where $|\mathcal{B}_n|$ represents the batch size, and r_k is the step size. We utilize the gradient descent algorithm, leveraging the gradient operator ∇ , to iteratively update the parameters. By scaling the gradient with the step size r_k and averaging it over the batch size $|\mathcal{B}_n|$, we

calculate the perturbation at each iteration. Through n iterations, we aim to find the maximum perturbation we desire.

Pretrained Teacher Module. After solving two challenging issues, we can easily interpret the first term of Equation (1). We employ a frozen pretrained T2M-GPT model as a teacher module. We aim to ensure consistency between SATO and the teacher model in predicting the original text. This is done to maintain the superior predictive performance of the original model while other modules enhance model stability during training, preventing the model from becoming overly stable and resulting in poor performance.

SATO Optimization Goal. we present our goal of SATO stable loss optimization as follows:

$$\min_{\tilde{w}} \mathbb{E}_x [\lambda_1 \underbrace{(D_2(\tilde{y}(x, \tilde{w}), y(x, w)))}_{\mathcal{L}_1} + \lambda_2 \underbrace{\mathcal{L}_{\text{Topk}}(\tilde{\omega}, \bar{\omega})}_{\mathcal{L}_2} + \lambda_3 \underbrace{(D_1(\tilde{y}(x, \tilde{\omega}), \tilde{y}(x, \bar{\omega}))}_{\mathcal{L}_3}] \quad (5)$$

Here $\bar{\omega}$ represents the attention vector after perturbation (PGD or RSSR). In T2M-GPT (and likewise for other models), we incorporate the three mentioned losses as auxiliary attention stability losses into the original model transformer loss $\mathcal{L}_{\text{trans}}$ for fine-tuning. Eventually, we obtain:

$$\mathcal{L} = \mathcal{L}_{\text{trans}} + \lambda_1 \cdot \mathcal{L}_1 + \lambda_2 \cdot \mathcal{L}_2 + \lambda_3 \cdot \mathcal{L}_3 \quad (6)$$

4 Experiments

Datasets. We selected the mainstream text-to-motion datasets HumanML3D [8] and KIT-ML [27] for the evaluation of perturbed text generation and human pose generation. The purpose of the perturbation is to simulate the diversity of motion descriptions by different dimensions in the real scene. Therefore, we first define the perturbation of the motion descriptions as follows: (1) All substitutions should be randomized (different parts and number of sentences); (2) Ensure that the semantics of the motion description are consistent before and after the replacement, avoid the distraction of polysemous words; (3) There should be a clear perturbation before and after the description replacement.

In detail, we randomly select 20% of the data for each of the training, validation, and test sets of the HumanML3D dataset, respectively, analyze the replaceable words in them, and generalize the replaceable words based on their lexical properties, where the generalized categories are: nouns, adjectives, adverbs, and verbs. Then, We combine them with the context to construct a thesaurus of synonymous substitutions for each word in each lexical property and batch replacements by rules.

Our replacement rule is to traverse the word list for each motion description, randomly replacing words or verb phrases in the lexicon until two types of lexical properties have been replaced, resulting in a perturb motion description sentence. Here are some examples: (1) "A man flaps his arms like a chicken while bending up and down." is replaced with: "A human flaps his arms like a chicken while stooping up and down." (2) "A person walks forward on an angle to the right." is replaced with: "A man walks ahead on an angle to the right." The examples in the lexicon are: "finally, ultimately, eventually," "clap, applaud, handclap," and so on.

We also performed a quantitative analysis of substitution as shown in Table 4, in the HumanML3D dataset, 99.13% of the motion descriptions were perturbed, and the frequency of perturbation (number of perturbed words compared to the total number of words on that description) per description amounted to 25.08%. Similarly, 97.74% of the descriptions in the KIT-ML dataset were perturbed, and the average perturbation rate reached 31.73%, which shows that the perturbation level of this perturbation strategy is fully reflected in both datasets. While keeping high perturbation, the average cosine similarity of descriptions before and after perturbation reaches 94.57% in the HumanML3D dataset, and 93.97% in the KIT-ML dataset, which indicates that the semantics before and after perturbation have strong consistency.

Evaluation Metrics. In addition to the commonly utilized metrics such as Frechet Inception Distance (FID), R-Precision, Multimodal Distance (MM-Dist), and Diversity, which are employed by T2M-GPT [38], we have introduced two additional metrics based on Frechet Inception Distance to further assess the stability of the model. Additionally, we utilize Jensen-Shannon Divergence to evaluate the stability of the model's attention. Furthermore, human evaluation is employed to obtain accuracy and human preference results for the outputs generated by the model.

- **Frechet Inception Distance [10] (FID):** We can evaluate the overall motion quality by measuring the distributional difference between the high-level features of the motions.
- **Human Evaluation:** We conducted evaluations of each model's generated results in the form of a Google Form. We collected user ratings on motion prediction, which encompassed both the quality and correctness of the generated motions. Additionally, we analyzed user preferences for pose prediction. Further details will be discussed in section 4.2.
- **Jensen-Shannon Divergence [13] (JSD):** We use JSD (Jensen-Shannon Divergence) to calculate the difference in attention vectors before and after perturbation to assess the stability of attention.

Notely, to measure the stability of the model, we will use three different *FID* input calculation methods: (1) *FID*: the distribution distance between the motion generated from the original text and real motion. (2) *FID_p*: the distribution distance between the motion generated from text after paraphrasing and real motion. (3) *FID_D*: the distribution distance between the motion generated from the original text and the motion generated from the text after paraphrasing. Moreover, we also employ human evaluation for cross-dataset evaluation to further analyze the performance and stability of the model. For assessing the stability of model attention, we propose using JSD. A smaller JSD value indicates greater stability of attention under perturbation.

4.1 Experimental Setup

We adopt nearly identical settings for model architecture parameters as T2M-GPT or MoMask. Additionally, We set the batch size to 64 and utilize the AdamW [23] optimizer with hyperparameters $[\beta_1, \beta_2] = [0.9, 0.99]$. The total iteration is set to 100000 and the learning rate is $1e-4$, employing a linear warm-up schedule for training all models. We respectively set $\lambda_1, \lambda_2, \lambda_3$ to 0.1, 0.2, and 0.05. For perturbation, we set r_k to 0.01, the PGD step as 10, and

Dataset	Methods	Venue	$FID\downarrow$	$FID_P\downarrow$	$FID_D\downarrow$	R-Precision			MM-Dist \downarrow	Diversity \uparrow
						Top1 \uparrow	Top2 \uparrow	Top3 \uparrow		
HumanML3D	TM2T [9]	ECCV2022	1.501 \pm .017	3.909 \pm .039	1.418 \pm .035	0.424 \pm .003	0.618 \pm .003	0.729 \pm .002	3.467 \pm .011	8.589 \pm .076
	T2M [8]	CVPR2022	1.087 \pm .021	3.990 \pm .064	2.110 \pm .039	0.455 \pm .003	0.636 \pm .003	0.736 \pm .002	3.347 \pm .008	9.175 \pm .083
	MotionDiffuse [40]	TPAMI2024	0.630 \pm .001	2.435 \pm .067	1.549 \pm .032	0.491 \pm .001	0.681 \pm .001	0.782 \pm .001	3.113 \pm .001	9.410 \pm .049
	MDM [33]	ICLR2023	0.544 \pm .044	6.283 \pm .154	5.428 \pm .160	–	–	0.611 \pm .007	5.566 \pm .027	9.559 \pm .086
	T2M-GPT [38]	CVPR2023	0.141 \pm .005	1.754 \pm .004	1.443 \pm .004	0.492 \pm .003	0.679 \pm .002	0.775 \pm .002	3.121 \pm .009	9.722\pm.082
	MoMask [7]	CVPR2024	0.045\pm.002	0.969 \pm .030	1.068 \pm .029	0.521\pm.002	0.713\pm.002	0.807\pm.002	2.962\pm.008	9.962\pm.008
	SATO (T2M-GPT)	–	0.157 \pm .006	0.155\pm.007	0.021\pm.006	0.454 \pm .003	0.637 \pm .003	0.738 \pm .003	3.338 \pm .013	9.651 \pm .050
	SATO(MoMask)	–	0.065\pm.003	0.070\pm.002	0.010\pm.001	0.501\pm.002	0.697\pm.003	0.801\pm.003	3.024\pm.010	9.599 \pm .075

Table 1: Quantitative evaluation on the HumanML3D. \pm indicates a 95% confidence interval. SATO(T2M-GPT) refers to fine-tuning based on T2M-GPT to create SATO, and similarly, SATO(MoMask) refers to fine-tuning based on MoMask to create SATO. Red indicates the best result, while blue refers to the second best.

Dataset	Methods	Venue	$FID\downarrow$	$FID_P\downarrow$	$FID_D\downarrow$	R-Precision			MM-Dist \downarrow	Diversity \uparrow
						Top1 \uparrow	Top2 \uparrow	Top3 \uparrow		
KIT-ML	TM2T	ECCV2022	3.599 \pm .051	10.619 \pm .156	4.008 \pm .228	0.280 \pm .006	0.463 \pm .007	0.587 \pm .005	4.591 \pm .028	9.473 \pm .145
	T2M	CVPR2022	3.022 \pm .107	8.832 \pm .153	3.864 \pm .119	0.361 \pm .006	0.559 \pm .007	0.681 \pm .007	3.488 \pm .028	10.720 \pm .145
	MotionDiffuse	TPAMI2024	1.954 \pm .062	5.737 \pm .172	2.496 \pm .106	0.417 \pm .004	0.621 \pm .004	0.739 \pm .004	2.958 \pm .005	11.100\pm.143
	MDM	ICLR2023	0.497 \pm .021	7.631 \pm .217	8.334 \pm .226	–	–	0.396 \pm .004	9.191 \pm .022	10.847 \pm .109
	T2M-GPT	CVPR2023	0.514 \pm .029	2.756 \pm .023	2.894 \pm .016	0.416 \pm .006	0.627 \pm .006	0.745 \pm .006	3.007 \pm .023	10.921\pm.108
	MoMask	CVPR2024	0.204\pm.011	2.570 \pm .092	2.234 \pm .101	0.433\pm.007	0.656\pm.005	0.781\pm.005	2.779\pm.022	10.734 \pm .008
	SATO (T2M-GPT)	–	0.706 \pm .041	0.679\pm.041	0.090\pm.041	0.380 \pm .005	0.587 \pm .006	0.709 \pm .005	3.203 \pm .024	10.860 \pm .107
	SATO (MoMask)	–	0.234\pm.011	0.259\pm.010	0.056\pm.002	0.425\pm.006	0.649\pm.003	0.780\pm.002	2.801\pm.019	10.499 \pm .090

Table 2: Quantitative evaluation on the KIT-ML. \pm indicates a 95% confidence interval. SATO (T2M-GPT) refers to fine-tuning based on T2M-GPT to create SATO, and similarly, SATO (MoMask) refers to fine-tuning based on MoMask to create SATO. Red indicates the best result, while blue refers to the second best.

Text	Model	Excellent (%)	Good (%)	Fair (%)	Poor (%)	Very poor (%)	Acc (%)	Preference (%)
Original text	T2M-GPT	27.0	29.0	20.5	18.0	5.5	76.5	53.5
	SATO (T2M-GPT)	29.0	26.5	22.5	16.0	6.0	78.0	
	MoMask	35.5	28.0	24.0	9.5	3.0	87.5	
	SATO (MoMask)	29.5	35.0	24.5	6.5	4.5	89.0	
Perturbed text	T2M-GPT	9.0	15.5	17.5	22.5	36.5	41.5	93.0
	SATO (T2M-GPT)	26.5	31.5	16.5	17.5	7.0	75.5	
	MoMask	11.0	14.5	24.0	14.5	35.0	49.5	
	SATO (MoMask)	22.0	27.5	32.0	12.0	6.5	81.5	
Cross Original text	T2M-GPT	51.5	19.5	16.0	10.5	2.5	87.0	67.0
	SATO (T2M-GPT)	55.5	23.0	15.5	5.0	1.0	94.0	
Cross Perturbed text	T2M-GPT	20.0	13.5	16.0	22.0	28.5	49.5	92.0
	SATO (T2M-GPT)	44.5	16.0	24.5	6.0	9.0	85.0	

Table 3: Human evaluation and cross-dataset results on the original or perturbed text. The cross-dataset evaluation result is that the model is trained on the HumanML3D dataset, with text from KIT-ML used for testing.

Dataset	Captions	Replacement Rate		Co-Sim (%)
		Caption (%)	Word (%)	
HumanML3D	87384	99.13	25.08	94.57
KIT-ML	12706	97.74	31.73	93.97

Table 4: Dataset analysis. We analyzed the replacement rates (sentences, vocabulary). Additionally, we calculated the cosine similarity (Co-Sim) before and after replacement to ensure the validity of our substitutions.

R to 0.05 when we use text embedding perturbation. Training can be conducted on a single RTX4090-24G GPU. It is worth noting that our method is based on fine-tuning the original model to make it more stable, without incurring any additional computation cost during the inference process.

4.2 Comparison with SOTA

Each experiment was repeated twenty times, and we reported the mean with a 95% statistical confidence interval. Tables 1 and 2 respectively present the results of models on the HumanML3D and KIT-ML datasets. We compare our results with six state-of-the-art (SOTA) methods.

Stability. It is worth noting that all other models perform poorly on the perturbed dataset, with FID_P significantly greater than FID , indicating that diverse representations of perturbations are fatal to the performance of these models. On FID_P , SATO (T2M-GPT) significantly reduced by 1.599 and 2.077 on HumanML3D and KIT-ML respectively, while SATO (MoMask) decreased by 0.899 and 2.311 respectively. Similarly, there was a significant increase in FID_D , with SATO (T2M-GPT) decreasing by 1.422 and 2.804 respectively, and SATO (MoMask) decreasing by 1.058 and 2.178 respectively. This suggests that **SATO yields similar predictive results on both perturbed and original datasets, indicating stronger stability.** We can also observe a significant reduction in the fluctuation of our model on the FID , FID_P , FID_D metrics, which also reflects the stability of our approach in predictions. We further investigated the impact of our approach on the attention JSD metric. Our method exhibits stability in attention, as evidenced by experiments and visualizations provided in the supplementary material.

Accuracy. Although our model experiences a slight decrease in FID and R-precision, we would like to point out that previous work

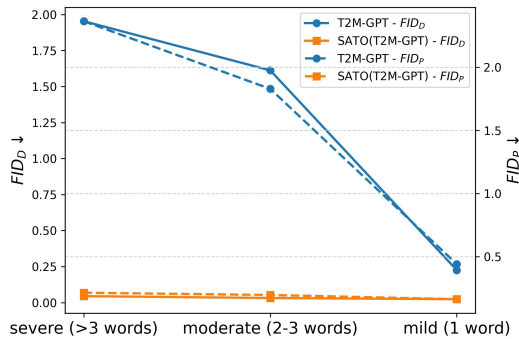


Figure 5: Model stability evaluation under different perturbations. It can be observed that across all levels of perturbation, SATO (T2M-GPT) consistently outperforms T2M-GPT in terms of stability metrics. Even when subjected to significant perturbation, our model maintains excellent stability.

has shown that a small decrease in FID does not necessarily imply a decrease in generation quality [14]. Furthermore, compared to the significant improvement in stability measured by the FID metric, the slight decrease in FID on the original text can be almost disregarded. Our visualizations and additional human evaluation experiments also demonstrate that the quality of text generated by our model on both original and perturbed text is superior to the original model. This means that textbfour model can generate higher-quality motion sequence outputs in practical applications, with a lower likelihood of catastrophic errors occurring when presented with a broader range of textual inputs.

Human Evaluation on the Original or Perturbed Text. Our work’s motivation is to address the catastrophic errors users encounter when using perturbed text by implementing a stable attention model. We further conduct a user study on Google Forms to validate the correctness of the model’s generation. We generated 200 motions for each method using the same text pool from the HumanML3D test set as the input for all baseline models and SATO. We set up questions for users to rate the motions. Table 3 shows that SATO not only maintains or even achieves better accuracy on the original text but also ensures stability when the text is perturbed. User preferences indicate that SATO performs slightly better than the original model on the original text and significantly outperforms the original model on the perturbed text dataset. More details can be found in the supplementary material.

Cross dataset evaluation. To further test and evaluate the robustness and applicability of our model, we compare SATO (T2M-GPT) with T2M-GPT as examples. We conducted training on the HumanML3D dataset, using 200 original and perturbed texts from the sample kit dataset as inputs for evaluation. Table 3 illustrates that SATO (T2M-GPT) achieves higher accuracy than the baseline by 7% on original texts and by 35.5% on perturbed datasets. Evaluators also tend to favor the quality of outputs generated by SATO. Both metrics indicate that our model demonstrates strong robustness to dataset variations. This also suggests that our approach can enhance the model’s generalization performance, enabling it to be applied in a wider range of domains.

Overall, SATO achieves state-of-the-art stability, balancing accuracy and robustness, resolving catastrophic errors caused by synonymous perturbations.

4.3 Ablation study

Ablation Study of SATO Stability Components. We conduct experiments on HumanML3D to evaluate the enhancements provided by our various modules in SATO, based on T2M-GPT. In Table 5, we observe that both the Stable Attention Module (\mathcal{L}_2) and Perturbation Module (\mathcal{L}_3) contribute to improving stability, as evidenced by the enhancements in FID_P by 1.521, 1.533 respectively, and FID_D by 1.417, 1.422 respectively. The combined effect of these modules achieves optimal stability performance.

Including the pre-trained Teacher Module (\mathcal{L}_1) enhances the model’s FID performance, preventing excessive stability at the expense of accuracy, albeit with a potential slight decrease in stability metrics. Moreover, this module plays a crucial role by automating the selection of the best training iterations, striking a balance between robustness and accuracy, and keeping the model more evenly poised between stability and accuracy.

Resistance to synonymous perturbation. Based on the varying numbers of synonymous word substitutions in the test set, we categorize perturbations as mild (1 word), moderate (2-3 words), and severe (>3 words). Visualizing the results in Fig. 5, it’s apparent that our model demonstrates superior stability compared to T2M-GPT across varying levels of perturbation. **Even when faced with severe perturbations, SATO consistently maintains excellent stability.** Our model’s stability metrics significantly outperform those of the original model on datasets with mild perturbations, underscoring its robustness across various degrees of perturbation.

5 CONCLUSION

We identified instability issues in the text-to-motion task and introduced a novel framework to address them. In the process of building SATO, we tackled two key challenges. We also proposed evaluation metrics for this task and constructed a dataset of 55k perturbed text pairs. Our experiments demonstrate that SATO is an attention-stable and prediction-robust framework, exhibiting broad applicability across various baselines and datasets. We aim to encourage more researchers to delve into this issue, further enhancing the performance and stability of text-to-motion systems.

\mathcal{L}_1	\mathcal{L}_2	\mathcal{L}_3	FID	FID_P	FID_D
✓	×	×	0.149	1.762	1.431
×	✓	×	0.187	0.221	0.026
×	×	✓	0.213	0.233	0.021
✓	✓	×	0.162	0.173	0.017
✓	×	✓	0.159	0.383	0.164
×	✓	✓	0.198	0.168	0.012
✓	✓	✓	0.157	0.155	0.010

Table 5: Ablation study results of SATO stability component. We conducted six separate ablation studies on three different loss functions. Bold indicates the best results.

A Overview of Supplementary Material

The supplementary material is organized into the following sections:

- Section B: Evaluation metrics.
- Section C: More visualization examples, including visual comparisons between SATO and state-of-the-art approaches, and attention visual examples.
- Section D: More ablation study, including parameter analysis, perturbation method ablation, and attention analysis.
- Section E: Details of human evaluation.
- Section F: SATO pseudo-algorithm.
- Section G: Computational complexity.
- Section H: Symbolic representation.

B EVALUATION METRICS

We denote the motion features generated from the original text and perturbed text as f_{pred} and f'_{pred} , respectively. The ground-truth motion features and text features are denoted as f_{gt} and f_t .

FID-related. FID is used to measure the difference in distribution between generated motions. We have the following formulas to obtain FID , FID_P , FID_D :

$$FID = \|\mu_{gt} - \mu_{pred}\|_2^2 - \text{Tr}(\Sigma_{gt} + \Sigma_{pred} - 2(\Sigma_{gt}\Sigma_{pred})^{1/2}) \quad (7)$$

$$FID_P = \|\mu_{gt} - \mu_{pred'}\|_2^2 - \text{Tr}(\Sigma_{gt} + \Sigma_{pred'} - 2(\Sigma_{gt}\Sigma_{pred'})^{1/2}) \quad (8)$$

$$FID_D = \|\mu_{pred} - \mu_{pred'}\|_2^2 - \text{Tr}(\Sigma_{pred} + \Sigma_{pred'} - 2(\Sigma_{pred}\Sigma_{pred'})^{1/2}) \quad (9)$$

Here, μ represents the mean, Σ is the covariance matrix, and Tr denotes the trace of a matrix. $pred$ denotes the prediction with the original text as input, and $pred'$ denotes the prediction with the perturbed text as input. FID and FID_P are metrics utilized to gauge the disparity in distribution between motions generated before and after perturbation, reflecting the variance between the generated motions and target motions. Meanwhile, FID_D evaluates the dissimilarity in generated motions pre- and post-perturbation. The smaller the difference, the less susceptible the model is to perturbation.

MM-Dist. MM-Dist quantifies the disparity between text embeddings and generated motion features. For N randomly generated samples, MM-Dist calculates the average Euclidean distance between each text feature and the corresponding motion feature, thus assessing feature-level dissimilarities between text and motion. Increasingly smaller MM-Dist values correspond to better prediction results.

$$\text{MM-Dist} = \frac{1}{N} \sum_{i=1}^N \|f_{pred,i} - f_{text,i}\| \quad (10)$$

Diversity. Diversity can measure the diversity of action sequences. A larger value of the metric indicates better diversity in the model. We randomly sample S pairs of motions, denoted as f_i and f'_i . According to [38], we set S to be 300. We can calculate using the following formula:

$$\text{Diversity} = \frac{1}{S} \sum_{i=1}^S \|f_i - f'_i\| \quad (11)$$

Jensen-Shannon Divergence (JSD). JSD can measure the similarity between two distributions, with values ranging from 0 to 1. Here, we utilize it to quantify the stability of attention before and after perturbation. We have the attention distributions before and after perturbation, denoted as $\tilde{\omega}$ and $\bar{\omega}$ respectively, computed as follows:

$$JSD(\tilde{\omega}, \bar{\omega}) = \frac{1}{2}KL[\tilde{\omega} || \frac{\tilde{\omega} + \bar{\omega}}{2}] + \frac{1}{2}KL[\bar{\omega} || \frac{\tilde{\omega} + \bar{\omega}}{2}] \quad (12)$$

where KL is the KL divergence between two distributions. A smaller JSD implies a stronger resistance of the model's attention to disturbances.

C MORE VISUALIZATION EXAMPLES

Visual Comparison between SATO and state-of-the-art approaches. As shown in Fig. 6, we randomly select perturbed text examples from the test set and visualize the predictions obtained from model inputs before and after perturbation. In both of these examples, SATO yielded correct predictions, while the other models encountered catastrophic failure issues. Our approach demonstrates consistent outputs and exhibits good stability before and after perturbation.

Attention visual examples. Fig. 7 illustrates the differences in attention between SATO and the original model before and after perturbation. The specific attention calculation method can be found in Section 3.1 of the main text. Across various examples, it is evident that the Jensen-Shannon Divergence (JSD) between text attention vectors before and after perturbation is significantly lower for SATO compared to the original model. The original model exhibits attention shifts when encountering synonymous perturbations, while SATO demonstrates better stability against synonymous perturbations across multiple examples.

D More ablation study

Parameters analysis. To explore the reasonable range of parameters for the loss function, we conducted 13 experiments on the SATO (T2M-GPT) model using the HumanML3D dataset, with three different loss settings. The results are shown in Table 8. Here, \mathcal{L}_1 , \mathcal{L}_2 , and \mathcal{L}_3 in the text represent the same losses. By fine-tuning the parameter ranges, we observed that slight increases or decreases in all loss parameters have little impact on the overall performance of the model. This is because, during the fine-tuning process, the three losses enable the model to dynamically balance towards stability and precision. For instance, when increasing \mathcal{L}_1 , we are more likely to obtain model weights that lean towards accuracy rather than stability. Upon analyzing the detailed changes, we found that the performance improvement in terms of FID and R-Top3 is associated with an increase in \mathcal{L}_1 , indicating its influence on model accuracy. On the other hand, the stability of the model is correlated with \mathcal{L}_2 and \mathcal{L}_3 , as reflected in the improvement of FID_P and FID_D when \mathcal{L}_2 and \mathcal{L}_3 are increased. Moreover, when we set large variations in the loss parameters, we observed that an excessively large \mathcal{L}_1 leads to higher accuracy but poor stability, while a too large \mathcal{L}_3 results in degraded performance due to excessive input perturbation during training, causing the model to lose its original good performance.

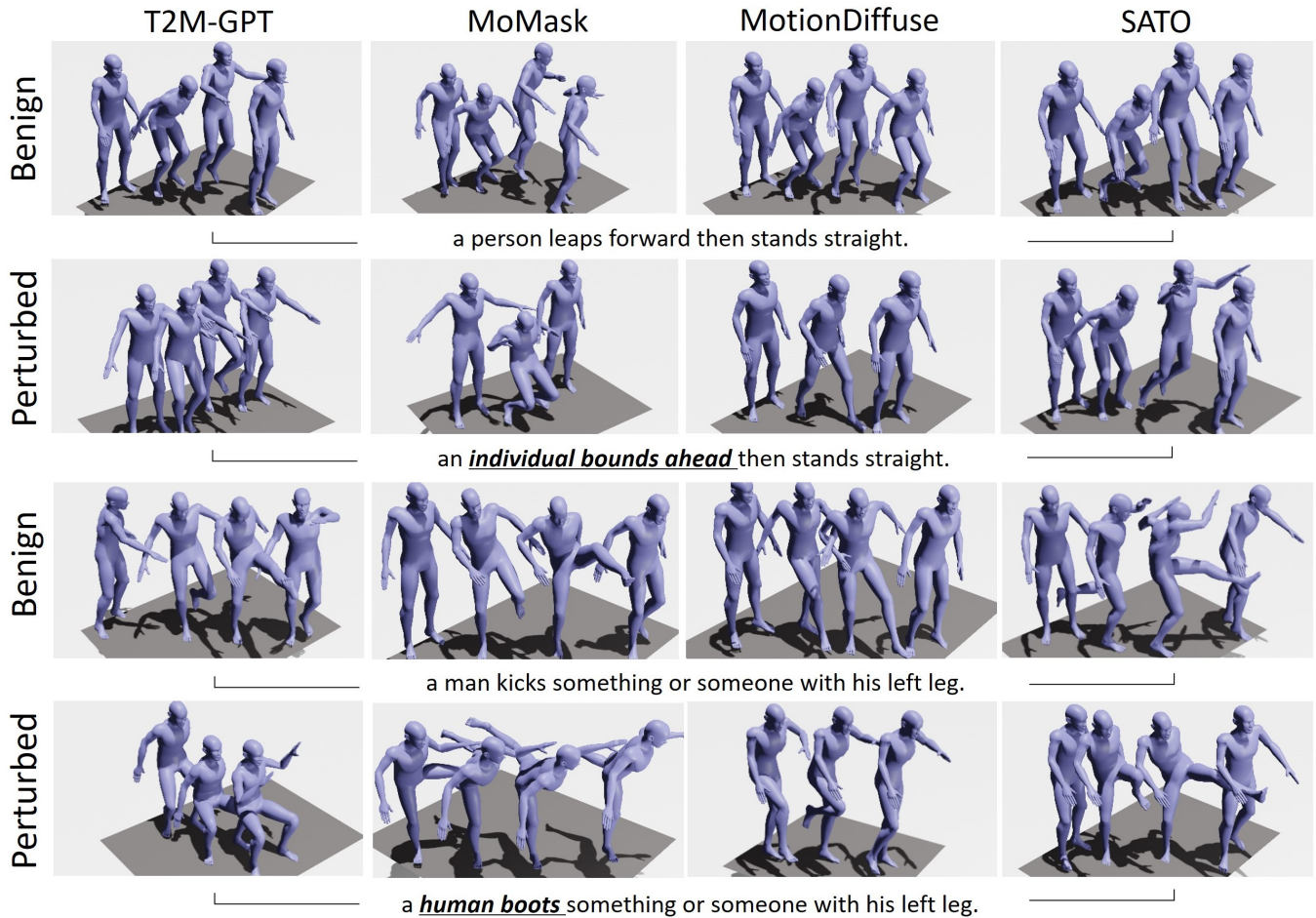


Figure 6: Visual comparison between SATO and state-of-the-art approaches. We compare SATO with T2M-GPT [38], MoMask [7], and MotionDiffuse [39]. We present two examples demonstrating predicted action sequences as outputs before and after perturbation. The underlined part is the part that scrambles the description. It can be observed that all models perform relatively accurately on the original text. However, only SATO predicts correctly on perturbed text.

Perturbation Method	Dataset	FID	FID_P	FID_D	JSD	$L_{feature}$
Without perturbation		0.141 \pm .005	1.754 \pm .004	1.443 \pm .004	0.228	33.657
PGD	HumanML3D	0.246 \pm .010	0.316 \pm .008	0.030 \pm .010	0.179	16.743
RSR		0.157 \pm .006	0.155 \pm .007	0.021 \pm .006	0.188	17.483

Table 6: Perturbation method ablation. We conducted ablation studies on SATO (T2M-GPT) using perturbation methods. "Without perturbation" refers to the original T2M-GPT model. JSD assesses the stability of the model's attention. $L_{feature}$ represents the L1 distance of the model's output text feature before and after perturbation. We have employed two methods to perturb the input, both of which significantly enhance model attention and prediction stability.

Perturbation method ablation. In the perturbation method section, we discussed two types of perturbation methods: PGD and RSR. To enhance the performance of PGD, we integrated data augmentation by randomly selecting either the original text or its synonym-disturbed counterpart as input. During training, we then

apply gradient-based perturbations to the selected input, generating the perturbed text. This approach differs from RSR, where the input comprises the original text, and its synonym-disturbed sentence serves as its perturbed text. Table 6 illustrates that both methods exhibited enhancements in FID_P and FID_D , with RSR showcasing superior stability. JSD highlighted the variance in text

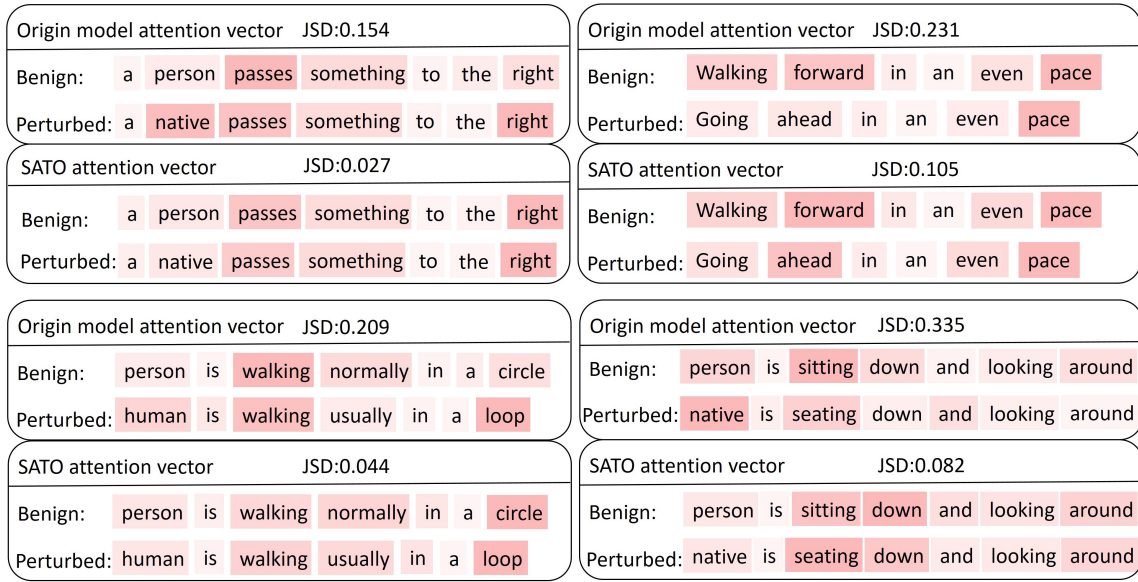


Figure 7: Attention visual examples. We compared the visualizations of attention vectors from the text encoder for T2M-GPT and SATO (T2M-GPT) before and after textual perturbations. In our visualizations, darker shades of red indicate higher attention weights. Additionally, we quantified the attention differences induced by perturbations using Jensen-Shannon Divergence (JSD). Our model exhibits a smaller JSD when the text is perturbed, indicating that our model possesses better attention stability.

Method	FID	FID_P	FID_D	JSD	Training time(h)	Inference time(s)
T2M-GPT	0.141 \pm .005	1.754 \pm .004	1.443 \pm .004	0.228	5.1	0.2557
Data augmentation	0.233 \pm .008	0.395 \pm .013	0.390 \pm .008	0.228	5.2	0.2557
SATO	0.157 \pm .006	0.155 \pm .007	0.021 \pm .006	0.188	12.6	0.2557

Table 7: Comparison with Data Augmentation: We conducted a comparison between SATO and the method of solely fine-tuning the model using data augmentation. The findings suggest that SATO exhibits superior accuracy and stability compared to relying solely on data augmentation.

attention before and after model perturbation. We observed that both methods enhanced the stability of text attention. Furthermore, we utilized L1 to gauge the disparity in text features outputted by the text encoder. It’s evident that after employing PGD or RSR, the outputted text features are significantly stabilized, which aids subsequent models in producing consistent outputs and thereby improving model stability. In this paper, we opted for the synonym replacement perturbation method, which exhibited superior stability and performance.

Compare with data augmentation. The instability of the Text-to-Motion model may stem from the limited diversity of vocabulary in the dataset, leading to poor generalization performance on unseen text. We conducted experiments using T2M-GPT as the base model on the HumanML3D dataset. We fine-tuned T2M-GPT using only data augmentation, where during training, we input randomly selected text either before or after synonymous perturbations, and compared it with SATO(T2M-GPT). In Table 7, our model exhibits better stability in attention, as evidenced by a significant decrease in JSD. Additionally, our model outperforms data augmentation methods on both the original dataset and the perturbed dataset, with

FID_P decreasing by 0.369, indicating better resistance to perturbations. In Fig. 6 and Fig. 8, we compare SATO (T2M-GPT) with the method of fine-tuning the original model using only data augmentation. From our randomly selected examples, we can observe that the results obtained solely through data augmentation still exhibit catastrophic errors. Combining quantification and visualization, we can conclude that the instability observed in the Text-to-Motion model does not solely stem from dataset limitations but also from attention instability. Consequently, solely relying on data augmentation is insufficient for mitigating the catastrophic errors induced by input perturbations.

Attention analysis. In the preceding sections, we employed JSD analysis to evaluate the stability of text encoders in SATO post fine-tuning, juxtaposing them against the original model’s text encoder. The results indicate SATO achieving the best JSD score (0.228 vs. 0.188). A noteworthy distinction between SATO and data augmentation lies in our adoption of a stable attention mechanism. While data augmentation falls short in stability metrics and visualization compared to SATO, this underscores the crucial role of the attention stability module in mitigating catastrophic model errors stemming from synonymous perturbations. Moreover, we observed a close correlation between the stability of outputted text features

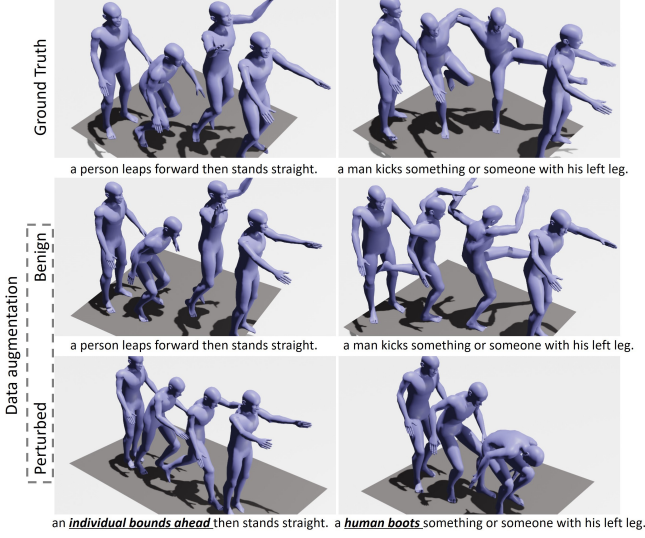


Figure 8: Visual examples of data augmentation methods. The first line is the ground truth of the motions. The second row shows the predictions of the data augmentation model on the original description, and the third line is on the perturbed description. The underlined part is the part that scrambles the description. Despite fine-tuning the original model with data augmentation, the visual results still indicate an inability to resolve catastrophic errors stemming from synonymous perturbations.

Algorithm 1 SATO

Input: Origin pre-trained Text-to-Motion model (e.g., T2M-GPT) $y(\cdot, \omega)$ and weight W ; Training data D including text data x and D' including perturbed text x' .

Initialize \hat{W} via W

if method == 'PGD' **then**

for $t = 1, 2, \dots, T$ **do**

 Initialize ρ_0^* .

for $n = 1, 2, \dots, N$ **do**

 Randomly sample a batch $\mathcal{B}_n \subset D$

$\rho_k = \rho_{k-1}^* + \frac{\eta}{|\mathcal{B}_n|} \sum_{x \in \mathcal{B}_n} \nabla (D_2(y(x, \hat{w}), y(x, \hat{w} + \rho_{k-1}^*)) + \mathcal{L}_{\text{Topk}}(\omega, \hat{\omega} + \rho_{k-1}^*))$

$\rho_k^* = \underset{\|\rho\| \leq R}{\text{argmin}} \|\rho - \rho_k\|$

end for

 Update \hat{W} using Stochastic Gradient Descent, where C_t is a batch, $\mathcal{L}_{\text{Trans}}$ is the loss of origin model

$\hat{W}_t = \hat{W}_{t-1} - \eta_t \sum_{x \in C_t} [\mathcal{L}_{\text{Trans}} + \lambda_1 D_2(\hat{y}(x, \hat{w}), y(x, w)) + \lambda_2 \mathcal{L}_{\text{Topk}}(\hat{\omega}, \hat{\omega} + \rho^*) + \lambda_3 D_1(\hat{y}(x, \hat{\omega}), \hat{y}(x, \hat{\omega} + \rho^*))]$

end for

else if method == 'RSR' **then**

 We get $\hat{\omega}$ from input x'

for $t = 1, 2, \dots, T$ **do**

 Update \hat{W} using Stochastic Gradient Descent, where C_t is a batch, $\mathcal{L}_{\text{Trans}}$ is the loss of origin model

$\hat{W}_t = \hat{W}_{t-1} - \eta_t \sum_{x \in C_t} [\mathcal{L}_{\text{Trans}} + \lambda_1 D_2(\hat{y}(x, \hat{w}), y(x, w)) + \lambda_2 \mathcal{L}_{\text{Topk}}(\hat{\omega}, \hat{\omega}) + \lambda_3 D_1(\hat{y}(x, \hat{\omega}), \hat{y}(x', \hat{\omega}))]$

end for

end if

return $\hat{W}^* = \hat{W}_T$

and attention stability. This suggests that SATO's resilience to perturbations in text encoder attention stabilizes the outputted text

features, thereby ensuring more consistent predictive outcomes in subsequent transformer structures.

E DETAILS OF HUMAN EVALUATION

[Question1]: Please evaluate the quality of the motion generation below.<motion1.gif>

- (1) Completely accurate semantically, with smooth and correct motion.
- (2) Generates well with minor details.
- (3) Some errors in detail, but overall correct.
- (4) Poor, mostly incorrect.
- (5) Very poor, completely incorrect semantically.

[Question2]: Please evaluate the quality of the motion generation below.<motion2.gif>

- (1) Completely accurate semantically, with smooth and correct motion.
- (2) Generates well with minor details.
- (3) Some errors in detail, but overall correct.
- (4) Poor, mostly incorrect.
- (5) Very poor, completely incorrect semantically.

[Question2]: Which motion result do you think is better?

- (1) The first one
- (2) The second one

We've employed the Google Form platform to enable 35 individuals to fill out multiple motion sequence tests independently. In total, there are 1200 questionnaires distributed. Our questionnaire design includes two types of questions. The first type involves directly rating the quality of generated motion. Motion is presented in GIF format, accompanied by five evaluation options: "Good" signifies generally well-generated motion with minor details; "Fair" indicates errors in details but overall correctness; "Poor" denotes overall incorrectness; and "Very poor" signifies motions and text that cannot be matched at all. We believe the first three options represent correctly generated postures, while the latter two represent errors. The second type of question pertains to user preferences between our model and a baseline model. This question compares our method and the original method from the user's perspective regarding motion generation accuracy.

F SATO Pseudo-Algorithm

The pseudo-algorithm for SATO is outlined in Algorithm 1.

G Computational complexity

During training, SATO incurs additional time due to the utilization of an extra frozen teacher model and the generation of predictions before and after output perturbation. Table 7 indicates that under the same experimental conditions (RTX4090-24G GPU), SATO (T2M-GPT) takes an additional 7.4 hours compared to T2M-GPT over 100,000 iterations. However, during the inference process, since SATO fine-tunes the original model without increasing the parameter count, it does not incur any additional time or space overhead. Table 7 also confirms this. When we use all the data from

\mathcal{L}_1	\mathcal{L}_2	\mathcal{L}_3	$FID\downarrow$	$FID_P\downarrow$	$FID_D\downarrow$	R-Top3 \uparrow
0.1	0.01	0.2	0.200 \pm .008	0.256 \pm .011	0.035 \pm .008	0.728 \pm .003
0.1	0.1	0.2	0.197 \pm .007	0.224 \pm .009	0.031 \pm .007	0.727 \pm .002
0.1	0.005	0.2	0.198 \pm .008	0.203 \pm .010	0.023 \pm .009	0.732 \pm .003
0.1	0.5	0.2	0.179 \pm .006	0.232 \pm .011	0.073 \pm .006	0.746 \pm .003
0.01	0.05	0.2	0.197 \pm .011	0.233 \pm .010	0.023 \pm .012	0.723 \pm .003
0.05	0.05	0.2	0.220 \pm .010	0.263 \pm .011	0.033 \pm .010	0.722 \pm .003
0.2	0.05	0.2	0.190 \pm .008	0.222 \pm .008	0.036 \pm .008	0.735 \pm .002
1.0	0.05	0.2	0.169 \pm .007	0.269 \pm .012	0.190 \pm .007	0.759 \pm .002
0.1	0.05	0.02	0.183 \pm .005	0.200 \pm .026	0.026 \pm .005	0.732 \pm .003
0.1	0.05	0.1	0.198 \pm .008	0.211 \pm .011	0.029 \pm .008	0.732 \pm .003
0.1	0.05	0.3	0.212 \pm .011	0.239 \pm .007	0.031 \pm .011	0.729 \pm .002
0.1	0.05	2.0	0.730 \pm .022	1.175 \pm .029	0.171 \pm .022	0.665 \pm .003
0.1	0.05	0.2	0.157 \pm .006	0.155 \pm .007	0.021 \pm .006	0.738 \pm .003

Table 8: Parameter analysis. \pm indicates a 95% confidence interval. R-top3 represents R-Precision Top3. The table displays the results of three different parameters for loss.

Notation	Remark	Notation	Remark
\mathbf{x}	input data	V_k	topk vector overlap ratio
$\omega, \tilde{\omega}$	attention vector, SATO attention vector	D	divergence metric
$\tilde{\omega}$	perturbed attention vector	\mathcal{W}	weight of text to motion model
\mathbf{X}	a pose sequence	$\mathbf{y}, \tilde{\mathbf{y}}$	prediction of text-to-motion model and SATO
C	a textual description	γ_1, γ_2, R	parameters in SATO
c_i	i^{th} word in the sentence	ρ	some perturbation
\mathcal{L}_{trans}	the loss of text-to-motion model	\mathcal{L}_{Topk}	a surrogate loss of $-V_k$
r_k	PGD step size	ζ_k^ω	top-k indices set of vector ω
\mathbf{e}	text embedding	$\lambda_1, \lambda_2, \lambda_3$	regularization parameters
\mathbf{t}	token index vector	\mathbf{e}	embedding weights
\mathbf{t}_e	text embedding vector	\mathbf{k}	key vector
\mathbf{q}	query vector	ω_t	attention weights

Table 9: Symbolic representation and remarks for the notation used in this paper.

HumanML3D as input with a batch size of 1, we obtain an average inference time of 0.2557 second per text.

H Symbolic representation

A table providing the symbolic representation employed throughout this paper is presented in Table 9. Each symbol is defined alongside its respective notation and meaning.

References

- [1] Tenglong Ao, Qingzhe Gao, Yuke Lou, Baoquan Chen, and Libin Liu. 2022. Rhythmic Gesticator: Rhythm-Aware Co-Speech Gesture Synthesis with Hierarchical Neural Embeddings. *ACM Transactions on Graphics* 41, 6 (Nov. 2022), 1–19. <https://doi.org/10.1145/3550454.3555435>
- [2] Nikos Athanasiou, Mathis Petrovich, Michael J. Black, and Gül Varol. 2022. TEACH: Temporal Action Composition for 3D Humans. arXiv:2209.04066 [cs.CV]
- [3] Pengxiang Cai, Zhiwei Liu, Guibo Zhu, Yunfang Niu, and Jinqiao Wang. 2024. Auto DragGAN: Editing the Generative Image Manifold in an Autoregressive Manner. arXiv:2407.18656 [cs.CV] <https://arxiv.org/abs/2407.18656>
- [4] Prafulla Dhariwal, Heewoo Jun, Christine Payne, Jong Wook Kim, Alec Radford, and Ilya Sutskever. 2020. Jukebox: A Generative Model for Music. arXiv:2005.00341 [eess.AS]
- [5] Patrick Esser, Robin Rombach, and Björn Ommer. 2021. Taming Transformers for High-Resolution Image Synthesis. arXiv:2012.09841 [cs.CV]
- [6] Anindita Ghosh, Noshaba Cheema, Cennet Oguz, Christian Theobalt, and Philipp Slusallek. 2021. Synthesis of Compositional Animations From Textual Descriptions. In *Proceedings of the IEEE/CVF International Conference on Computer Vision (ICCV)*. 1396–1406.
- [7] Chuan Guo, Yuxuan Mu, Muhammad Gohar Javed, Sen Wang, and Li Cheng. 2023. MoMask: Generative Masked Modeling of 3D Human Motions. arXiv:2312.00063 [cs.CV]
- [8] Chuan Guo, Shihao Zou, Xinxin Zuo, Sen Wang, Wei Ji, Xingyu Li, and Li Cheng. 2022. Generating Diverse and Natural 3D Human Motions From Text. In *Proceedings of the IEEE/CVF Conference on Computer Vision and Pattern Recognition (CVPR)*. 5152–5161.
- [9] Chuan Guo, Xinxin Zuo, Sen Wang, and Li Cheng. 2022. TM2T: Stochastic and Tokenized Modeling for the Reciprocal Generation of 3D Human Motions and Texts. arXiv:2207.01696 [cs.CV]
- [10] Martin Heusel, Hubert Ramsauer, Thomas Unterthiner, Bernhard Nessler, and Sepp Hochreiter. 2018. GANs Trained by a Two Time-Scale Update Rule Converge to a Local Nash Equilibrium. arXiv:1706.08500 [cs.LG]
- [11] Lijie Hu, Yixin Liu, Ninghao Liu, Mengdi Huai, Lichao Sun, and Di Wang. 2022. SEAT: Stable and Explainable Attention. arXiv:2211.13290 [cs.CL]
- [12] Lijie Hu, Yixin Liu, Ninghao Liu, Mengdi Huai, Lichao Sun, and Di Wang. 2024. Improving Interpretation Faithfulness for Vision Transformers. arXiv:2311.17983 [cs.CV] <https://arxiv.org/abs/2311.17983>
- [13] Sarthak Jain and Byron C. Wallace. 2019. Attention is not Explanation. arXiv:1902.10186 [cs.CL]
- [14] Sadeep Jayasumana, Srikumar Ramalingam, Andreas Veit, Daniel Glasner, Ayan Chakrabarti, and Sanjiv Kumar. 2024. Rethinking FID: Towards a Better Evaluation Metric for Image Generation. arXiv:2401.09603 [cs.CV]
- [15] Peng Jin, Yang Wu, Yanbo Fan, Zhongqian Sun, Yang Wei, and Li Yuan. 2023. Act As You Wish: Fine-Grained Control of Motion Diffusion Model with Hierarchical Semantic Graphs. In *NeurIPS*.
- [16] Hyunjae Kim, Seunghyun Yoon, Trung Bui, Handong Zhao, Quan Tran, Franck Deroncourt, and Jaewoo Kang. 2024. Fine-tuning CLIP Text Encoders with Two-step Paraphrasing. arXiv:2402.15120 [cs.CV]
- [17] Shunsuke Kitada and Hitoshi Iyatomi. 2021. Attention Meets Perturbations: Robust and Interpretable Attention With Adversarial Training. *IEEE Access* 9 (2021), 92974–92985. <https://doi.org/10.1109/ACCESS.2021.3093456>
- [18] Songning Lai, Lijie Hu, Junxiao Wang, Laure Berti-Equille, and Di Wang. 2024. Faithful Vision-Language Interpretation via Concept Bottleneck Models. In *The Twelfth International Conference on Learning Representations*. <https://openreview.net/forum?id=rp0Edl8X4e>
- [19] Jia Li, Lijie Hu, Jingfeng Zhang, Tianhang Zheng, Hua Zhang, and Di Wang. 2024. Fair Text-to-Image Diffusion via Fair Mapping. arXiv:2311.17695 [cs.CV] <https://arxiv.org/abs/2311.17695>
- [20] Jiawei Lin, Zhaoyun Jiang, Jiaqi Guo, Shizhao Sun, Ting Liu, Zijiang James Yang, Jian-Guang Lou, and Dongmei Zhang. 2024. IconDM: Text-Guided Icon Set Expansion Using Diffusion Models. In *ACM Multimedia 2024*. <https://openreview.net/forum?id=SsVvRdheMH>
- [21] Ting Liu, Xuyang Liu, Siteng Huang, Honggang Chen, Quanjun Yin, Long Qin, Donglin Wang, and Yue Hu. 2024. DARA: Domain-and Relation-aware Adapters Make Parameter-efficient Tuning for Visual Grounding. *arXiv preprint arXiv:2405.06217* (2024).
- [22] Xuyang Liu, Siteng Huang, Yachen Kang, Honggang Chen, and Donglin Wang. 2024. Vgdiffzero: Text-to-image diffusion models can be zero-shot visual grounders. In *ICASSP 2024-2024 IEEE International Conference on Acoustics, Speech and Signal Processing (ICASSP)*. IEEE, 2765–2769.
- [23] Ilya Loshchilov and Frank Hutter. 2019. Decoupled Weight Decay Regularization. arXiv:1711.05101 [cs.LG]
- [24] Aleksander Madry, Aleksandar Makelev, Ludwig Schmidt, Dimitris Tsipras, and Adrian Vladu. 2019. Towards Deep Learning Models Resistant to Adversarial Attacks. arXiv:1706.06083 [stat.ML]
- [25] Mathis Petrovich, Michael J. Black, and Gül Varol. 2021. Action-Conditioned 3D Human Motion Synthesis with Transformer VAE. arXiv:2104.05670 [cs.CV]
- [26] Mathis Petrovich, Michael J. Black, and Gül Varol. 2022. TEMOS: Generating diverse human motions from textual descriptions. arXiv:2204.14109 [cs.CV]
- [27] Matthias Plappert, Christian Mandery, and Tamim Asfour. 2016. The KIT Motion-Language Dataset. *Big Data* 4, 4 (Dec. 2016), 236–252. <https://doi.org/10.1089/big.2016.0028>
- [28] Alec Radford, Jong Wook Kim, Chris Hallacy, Aditya Ramesh, Gabriel Goh, Sandhini Agarwal, Girish Sastry, Amanda Askell, Pamela Mishkin, Jack Clark, Gretchen Krueger, and Ilya Sutskever. 2021. Learning Transferable Visual Models From Natural Language Supervision. arXiv:2103.00020 [cs.CV]
- [29] Aditi Raghunathan, Sang Michael Xie, Fanny Yang, John Duchi, and Percy Liang. 2020. Understanding and Mitigating the Tradeoff Between Robustness and Accuracy. arXiv:2002.10716 [cs.LG]
- [30] Aditya Ramesh, Mikhail Pavlov, Gabriel Goh, Scott Gray, Chelsea Voss, Alec Radford, Mark Chen, and Ilya Sutskever. 2021. Zero-Shot Text-to-Image Generation. arXiv:2102.12092 [cs.CV]
- [31] Motoki Sato, Jun Suzuki, Hiroyuki Shindo, and Yuji Matsumoto. 2018. Interpretable Adversarial Perturbation in Input Embedding Space for Text. In *Proceedings of the Twenty-Seventh International Joint Conference on Artificial Intelligence, IJCAI-18*. International Joint Conferences on Artificial Intelligence Organization, 4323–4330. <https://doi.org/10.24963/ijcai.2018/601>
- [32] Guy Tevet, Brian Gordon, Amir Hertz, Amit H. Bermano, and Daniel Cohen-Or. 2022. MotionCLIP: Exposing Human Motion Generation to CLIP Space. arXiv:2203.08063 [cs.CV]
- [33] Guy Tevet, Sigal Raab, Brian Gordon, Yonatan Shafir, Daniel Cohen-Or, and Amit H. Bermano. 2022. Human Motion Diffusion Model. arXiv:2209.14916 [cs.CV]
- [34] Aaron van den Oord, Oriol Vinyals, and Koray Kavukcuoglu. 2018. Neural Discrete Representation Learning. arXiv:1711.00937 [cs.LG]
- [35] Yin Wang, Zhiying Leng, Frederick W. B. Li, Shun-Cheng Wu, and Xiaohui Liang. 2023. Fg-T2M: Fine-Grained Text-Driven Human Motion Generation via Diffusion Model. arXiv:2309.06284 [cs.CV] <https://arxiv.org/abs/2309.06284>
- [36] Will Williams, Sam Ringer, Tom Ash, John Hughes, David MacLeod, and Jamie Dougherty. 2020. Hierarchical Quantized Autoencoders. arXiv:2002.08111 [cs.LG]
- [37] Hongyang Zhang, Yaodong Yu, Jiantao Jiao, Eric Xing, Laurent El Ghaoui, and Michael Jordan. 2019. Theoretically Principled Trade-off between Robustness and Accuracy. In *Proceedings of the 36th International Conference on Machine Learning (Proceedings of Machine Learning Research, Vol. 97)*, Kamalika Chaudhuri and Ruslan Salakhutdinov (Eds.). PMLR, 7472–7482. <https://proceedings.mlr.press/v97/zhang19p.html>
- [38] Jianrong Zhang, Yangsong Zhang, Xiaodong Cun, Shaoli Huang, Yong Zhang, Hongwei Zhao, Hongtao Lu, and Xi Shen. 2023. T2M-GPT: Generating Human Motion from Textual Descriptions with Discrete Representations. arXiv:2301.06052 [cs.CV]
- [39] Mingyuan Zhang, Zhongang Cai, Liang Pan, Fangzhou Hong, Xinying Guo, Lei Yang, and Ziwei Liu. 2022. MotionDiffuse: Text-Driven Human Motion Generation with Diffusion Model. arXiv:2208.15001 [cs.CV]
- [40] Mingyuan Zhang, Zhongang Cai, Liang Pan, Fangzhou Hong, Xinying Guo, Lei Yang, and Ziwei Liu. 2024. MotionDiffuse: Text-Driven Human Motion Generation With Diffusion Model. *IEEE transactions on pattern analysis and machine intelligence* PP (01 2024). <https://doi.org/10.1109/TPAMI.2024.3355414>
- [41] Mingyuan Zhang, Xinying Guo, Liang Pan, Zhongang Cai, Fangzhou Hong, Huirong Li, Lei Yang, and Ziwei Liu. 2023. ReMoDiffuse: Retrieval-Augmented Motion Diffusion Model. arXiv:2304.01116 [cs.CV]
- [42] Yiran Zhao, Wenyue Zheng, Tianle Cai, Xuan Long Do, Kenji Kawaguchi, Anirudh Goyal, and Michael Shieh. 2024. Accelerating Greedy Coordinate Gradient via Probe Sampling. arXiv:2403.01251 [cs.CL]